ISSN 1062-8738, Bulletin of the Russian Academy of Sciences: Physics, 2019, Vol. 83, No. 5, pp. 591–595. © Allerton Press, Inc., 2019.
Russian Text © The Author(s), 2019, published in Izvestiya Rossiiskoi Akademii Nauk, Seriya Fizicheskaya, 2019, Vol. 83, No. 5, pp. 650–654.

Continuous Glow of the Nighttime Atmosphere during Thunderstorms and the Dynamics of Its Electrical State, Derived from Data on Cosmic Ray Variations

N. S. Khaerdinov[a], *, A. S. Lidvansky[a], and M. N. Khaerdinov[a]

[a] *Institute for Nuclear Research, Russian Academy of Sciences, Moscow, 117312 Russia*

**e-mail: khaerdinovns@yandex.ru*

Received September 15, 2018; revised November 6, 2018; accepted January 28, 2019

Abstract—New physical effects accompanying thunderstorms are studied at the Baksan Neutrino Observatory with the Carpet air shower array. Techniques are developed that allow the potential difference in the troposphere to be estimated using data on the variations in secondary cosmic rays. Remote digital video cameras continuously observe the night sky above the array. The means of analysis is described, and some experimental evidence is presented for correlations between the high-altitude glow and variations in the detected particle flux and global disturbances of the geomagnetic field. Examples of the possible influence of seismic activity on the dynamics of thunderstorms are presented.

DOI: 10.3103/S1062873819050162

INTRODUCTION

Some examples of the night sky's continuous glow above thunderstorm clouds were presented in [1–3]. They were recorded as a result of a comprehensive study of the effects that accompany the slow electric breakdown of the stratosphere, initiated by avalanches of runaway electrons. The existence of large amplitude (around 1%) variations in muons, detected integrally over all angles, was a precondition for considering such events. In [4, 5], a technique was described that allows us to estimate the potential difference in the troposphere above the Carpet array by analyzing variations in the intensity of the inclined muons it records. The same technique allows us to investigate field variations in thunderclouds with bipolar distributions of charge. One such thunderstorm event is analyzed below.

EXPERIMENTAL

The Carpet air shower array at the Baksan Neutrino Observatory (43.3° N, 42.7° E) of the Institute for Nuclear Research (Moscow) is located in a mountain valley at an altitude of 1.7 km a.s.l. The count rates of secondary cosmic ray particles are measured uninterruptedly, along with atmospheric pressure, temperature, the near-ground electric field, and the precipitation electric current. All detected particles can be separated into soft and hard components. After a correction procedure, two independent channels of secondary cosmic ray particles propagating through the atmosphere are used in the experiment: the electron–photon and muon components. In [4], an experimental technique was described that allows us to measure with the Carpet array variations in the intensity of inclined muons during thunderstorms. The technique is based on more inclined particles producing greater amplitudes in the summed signal of individual detectors when recording muons with a horizontal layer of scintillation detectors (a square of 400 scintillators, each of which has dimensions of $70 \times 70 \times 30$ cm^3). Dividing all detected muons in three groups according to their energy release, we can identify three angular zones and radial borders of the vertical field region corresponding to them: vertical muons (30–62 MeV or 0°–37°, 0–3.5 km), intermediate muons (62–90 MeV or 37°–56°, 3.5–12 km), and peripheral muons (more than 90 MeV) $\leftrightarrow$ 56°, more than 12 km. Applying the theory of cosmic ray variations being created by an electric field, this procedure allows us [5] to estimate a bipolar field distribution in the horizontal plane, determining the vertical field potential difference above the array and at the periphery at distances of more than 12 km. This way of estimating fields assumes a stable temperature in the atmosphere. The results from calculations are correct for rapid variations, during which changes in temperature are negligible. Two remote points of video observation cover the region of sky above the array from distances of 0.5 km (Neutrino point, the main direction to the south) and 75 km (Khasanya village, the main direction to the west), respectively. Every point makes observations using two cameras in the color and infrared modes. The procedure for processing the video data was described in [2].

This work presents data recorded with black-and-white resolution by Cs265 video cameras in the nighttime mode. In order to separate the glow according to altitude, a full frame is divided into three equal horizontal regions: upper (ionosphere), middle (stratosphere), and lower (troposphere). For comparison to the background, a photo being processed is divided into three equal vertical zones: left, right, and central. When making quantitative analyses, the average brightness of pixels is determined for local regions on the photo. Direct calibration with light sources of different colors is performed to establish the functional connection between the brightness of a remote continuous surface and the mean pixel brightness of its image on the photo.

RESULTS AND DISCUSSION

Figure 1 presents the results from a comprehensive study of a thunderstorm event that occurred on the night of July 24–25, 2014. The local time, which is 3 h ahead of Universal Time, is used everywhere in this work. Negatively charged rain started at 21:00 against a background of declining atmospheric pressure and near-ground temperature. The electric field did not exceed the instrument's level of sensitivity, showing that the thunderstorm began to develop far from the array. Throughout the night, no great variations were observed in the integral flux of muons. Repair work at the experimental facility continued until 21:00, influencing the stability of recording somewhat (there was a jump in intensity around 21:00). Time profiles were obtained for the potential differences above the array and at the periphery. A positive field disturbance in the troposphere was seen immediately after stopping the repair work, with no such effect being observed at the periphery. The corresponding disturbance of vertical muons was probably due to active cloud formation beginning above the array's position, as was seen in evening photos at earlier hours. Note that the last peak of this glow coincided both in time and shape with a positive global disturbance in the X-component of the geomagnetic field with maximum amplitude at 22:37. The magnetic field had been relatively quiet for three hours until this moment. A series of disturbances then occurred that transformed into a cascade of substorms, the first (greatest) of which began to expand at 02:25. Figure 1 thus presents the dynamics and electrical state of the nighttime atmosphere during a thunderstorm against a background of substorms developing in the magnetosphere.

Analysis of muon variations shows that from 23:30 on, a negative potential difference gradually started to form in the troposphere. At 00:56, the gradual increase in its amplitude above the array sharply changed into a drop with a subsequent reversal of polarity at 01:25. Such behavior is consistent with the model of a slow breakdown of the stratosphere, initiated by avalanches of runaway electrons that are accelerated into the ionosphere in a near-threshold regime by the negative charge of the thundercloud's top. As a result of this breakdown, the negative charge travels into the ionosphere, and the positive charge farther down now has to determine the potential difference in the troposphere. In the period where the charge changed above the array (01:03–01:22) the remote camera at Khasanya (75 km away) recorded a glow at a level of 10% above the background. Calibration showed the camera's background brightness E_b was 3×10^{-3} cd m^{-2}. The increased brightness of the upper part of the sky during the breakdown was thus $dE \approx 3 \times 10^{-4}$ cd m^{-2}. At 01:14, the glow reached its maximum brightness and became local with angular dimensions of around 20° × 20°. It then began to decay. In a visual analysis of the photos, we could clearly see a star in place of the glow in the region of the ionosphere before 01:03 and after 01:21. This means the glow was transparent in the initial period, and not during the rest of the time. Transparency returned after the end of the glow. The peripheral negative field continued to grow in parallel with the reversal of the thunderstorm field above the array. The star disappeared again at 01:40. From this moment on, the glow began to brighten over the width of the photo. The ionosphere glowed most. In Fig. 1, we can see a 100 MV disturbance of the positive potential difference in the troposphere above the array in the period 01:45–01:50. According

Fig. 1. Thunderstorm event of July 24–25, 2014, on the local time scale. Data is averaged over 10 s intervals, unless otherwise specified: (a) precipitation electric current; (b) atmospheric pressure; (c) near-ground air temperature; (d) strength of the near-ground electric field. (e) Brightness of the glow, as measured by a remote (75 km) video camera, with values using a different duty factor (exposure, 0.2 s); the upper line represents the mean brightness of the top area (the ionosphere) of the frame's central zone, while the lower line shows the brightness of the bottom area (the troposphere) of the central zone (for convenience, the plot is presented with a subtraction of 2 units); the ordinate axis presents data in units of $1 \sim 10^{-7}$ lx of camera objective illumination. (f) Variations in muon intensity with an energy release of 30–60 MeV (vertical muons) in detectors; (g) variations of muon intensity with energy release above 90 MeV (peripheral muons). (h) Data from the near (0.5 km) video camera; duty cycle, 30 s (exposure, 0.2 s). The upper line represents the mean brightness of the upper region (the ionosphere) of the entire frame; the middle line corresponds to the brightness of the middle region (the stratosphere; the plot is given with subtraction of 0.3 units); the lower line is the brightness of the lower region (the troposphere; the plot is given with a subtraction of 1.3 units) of the frame; the ordinate axis is in units of $1 \sim 10^{-7}$ lx illumination. (i) Variations of the X-component of geomagnetic field induction (northward) according to data from several mid-latitude stations (http://www.intermagnet.org) with 1 min averaging; the thick line is for the Borok station data (58.07° N, 38.23° E). (k) Moments of earthquakes with magnitudes greater than 1 over the globe (http://www.emsc-csem.org/Earthquake) (accuracy, 1 s). (l) Mean potential difference in the troposphere above the array (5 min averaging); (m) mean potential difference in the troposphere for the peripheral region (5 min averaging).

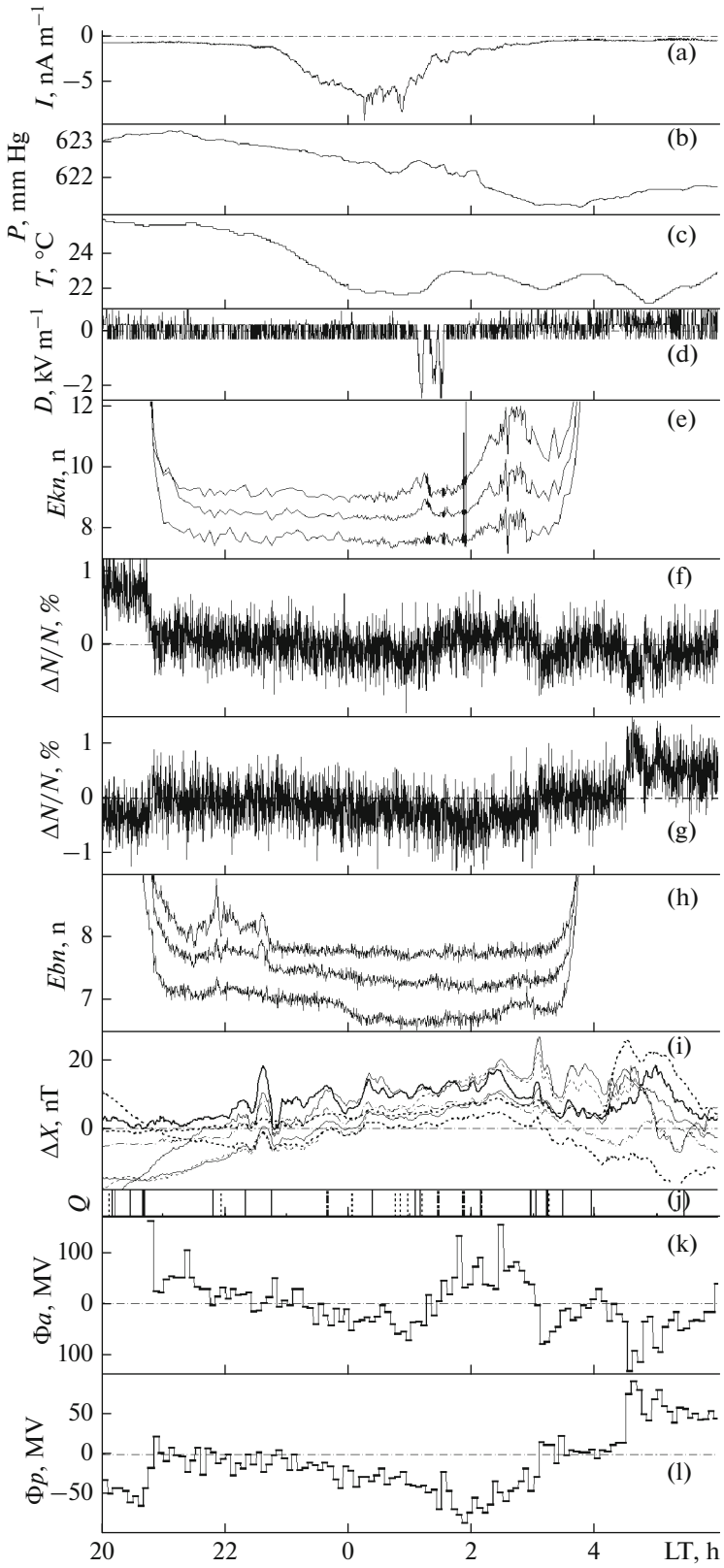
I, nA m⁻¹
0
−5
(a)
P, mm Hg
623
622
(b)
T, °C
24
22
(c)
D, kV m⁻¹
0
−2
(d)
Ekn, n
12
10
8
(e)
ΔN/N, %
1
0
(f)
ΔN/N, %
1
0
−1
(g)
Ebn, n
8
7
(h)
ΔX, nT
20
0
(i)
Q
(j)
Φa, MV
100
0
100
(k)
Φp, MV
50
0
−50
(l)
20
22
0
2
4
LT, h

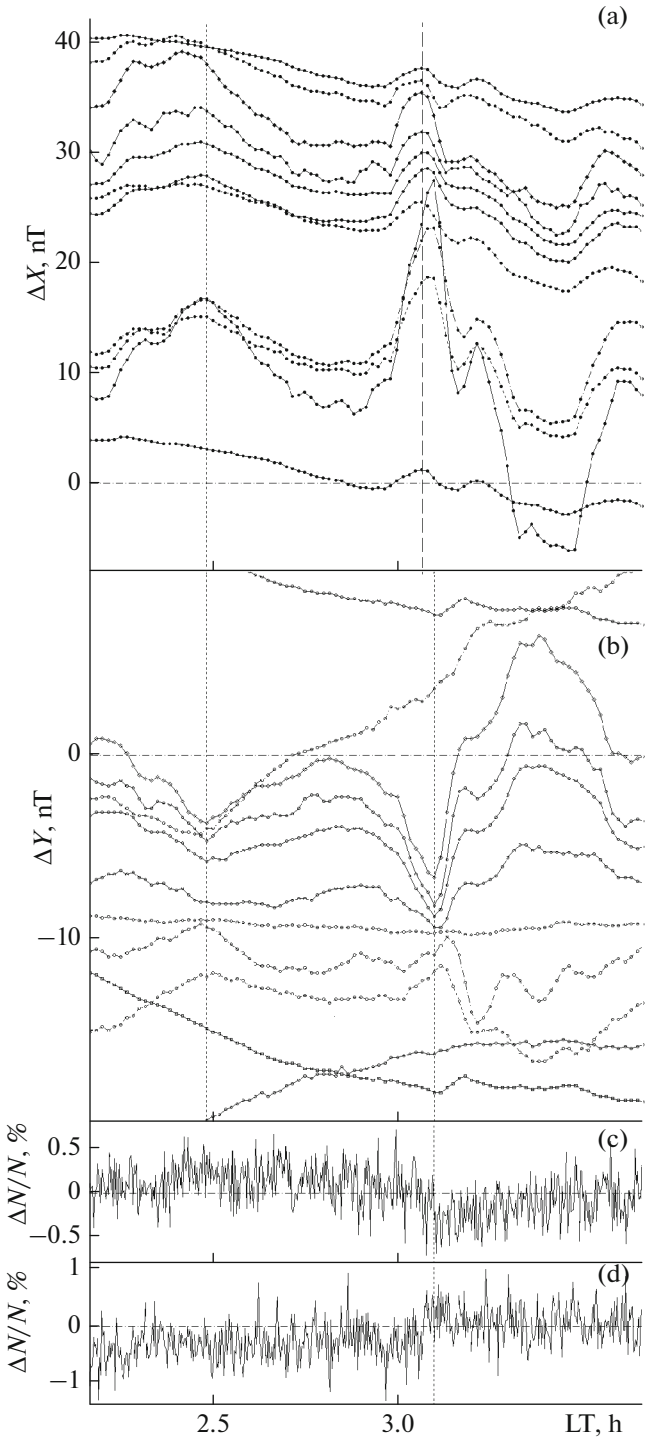

Fig. 2. Thunderstorm event of July 24–25, 2014. Variations in geomagnetic field induction are presented as measured by a network of mid-latitude geophysical stations (website http://www.intermagnet.org). Local time is used. For a better comparison of variations, the plots for each component and each station are displaced along the ordinate axis so they would be (if possible) higher than those of geographically more western stations. The upper and lower plots in the figure were obtained by shifting the data of a single station. The stations' coordinates are (from bottom to top) (1) 27.2° S, 250.58° E, IPM (Isla de Pascua Mataveri (Easter Island)); (2) 49.87° N, 260.0261° E, Brandon; (3) 38.2° N, 282.63° E, Fredericksburg; (4) 43.9321° N, 299.9905° E, Sable Island; (5) 22.4° S, 316.35° E, Vassouras; (6) 40.957° N, 0.333° E, Ebro; (7) 49.08° N, 14.02° E, Budkov; (8) 51.84° N, 20.79° E, Blesk; (9) 58.07° N, 38.23° E, Borok; (10) 43.2° N, 76.9° E, Alma Ata; (11) 27.2° S, 250.58° E, IPM. (a) Variations of the X component (northward) of geomagnetic field induction over the network of stations (averaging time, 1 min); (b) variations of the Y component (eastward) of the geomagnetic field over the global network stations (averaging time, 1 min); (c) variations in the intensity of muons with energy release in detectors in the range of 30–60 MeV (vertical muons; averaging time, 10 s); (d) variations of the intensity of muons with energy release in detectors of more than 90 MeV (peripheral muons; averaging time, 10 s).

to data from http://www.emsc-csem.org/Earthquake, an earthquake at a depth of 5 km with a magnitude of 3.3 was recorded at 01:51:05. Its distance from the site of the experiment was 315 km (43.31° N, 46.85° E). Two lightning discharges were recorded by video cameras above the mountains at 01:52:14 and 01:53:53. At 01:55, the gradual increase of the negative potential difference at the periphery transformed into a regular drop until its polarity reversed at 03:04. According to the model, a slow breakdown of the stratosphere began above the periphery. Another jump of the positive potential difference in the troposphere was recorded in the period 02:00–02:10. Two nearly simultaneous earthquakes were recorded at 02:09:17 and 02:09:04. The first one was relatively nearby in Turkey, at a distance of 1489 km (36.45° N, 27.11° E; depth and magnitude, 7 km and 2.4, respectively). Another 4.5 magnitude earthquake occurred in the Atlantic Ocean (28.6° N, 43.8° E; depth, 7 km). All this time, the brightness of the large-scale glow of the night sky grew continuously. The expansion phase of a magnetospheric substorm began at 02:29. This is clearly seen in the plot of geomagnetic field variations (Fig. 2) measured by mid-latitude stations with different longitudes. According to the description of the initial phase of magnetospheric substorm development [6, p. 94], if activation begins with a current discontinuity in the magnetotail, a substorm current wedge should appear that forms a westward electrojet in the ionosphere at an altitude of 100 km during the midnight hours (±2 h). It is usually located at the latitude of the auroral oval (60°) in a narrow interval where the activity of auroras during substorms is maximal. The Earth's magnetic field is in this case disturbed in a fairly specific way (as was described in [6], p. 104). We can see in the plots that there were two activations of different character in the period 02:10–03:40. During the first of these, moments of extreme values in variations of the Y component coincided for all stations. The substantial difference observed in the second event was the onset of pulsations. Note that in the first case (02:29), as in that of the earthquake, a spike of positive potential difference in the troposphere above the array

was recorded at the initial moment of substorm development (02:25–02:30), bringing the brightness of the glow to its maximum value. A pulsed discharge occurred during the second activation (03:40). The jump in potential difference at the periphery lasted for 30 s. It is likely that this second activation was accompanied by a positive field jump, resulting in a high-altitude discharge in the region of the negatively charged periphery. Large numbers of accelerated runaway electrons escaped into the magnetosphere, thus compensating for the positive potential spike. These initiated an eastward drift, producing a negative disturbance in the field's X component during their propagation. This is clearly seen in the upper panel of Fig. 2. For example, a local minimum in the X component for the Alma-Ata station (43.2° N, 76.9° E) located 30 degrees to the east occurred at 03:07, earlier than for other stations. For station IPM (27.2° S, 250.58° E; Isla de Pascua Mataveri (Easter Island)), the delay was 3 min. The mean energy of particles drifting with this velocity was 9 MeV for our latitude. At 03:06, the intensity of vertical muons fell sharply, corresponding to the emergence of a negative field above the array, the periphery field being constant at the same time. The glow ended later. This moment (03:06) coincided with the time of the Y component's local extremum over the morning part of the Earth. Note that a considerable negative disturbance in the X component began to increase at the Brandon station (49.8° N, 260.0261° E), interrupting its prolonged growth without changing the field in the eastern direction (Y). This means the considered effect was local in the ring current and resulted in stabilization of the magnetic field.

CONCLUSIONS

A continuous diffuse glow of the night sky is recorded above thunderclouds. It accompanies the dynamic period of a reversal of the electric field in the troposphere from negative to positive. The glow at maximum is opaque with an amplitude of 3×10^{-4} cd m^{-2}, its dimensions are 20° × 20°, and its center is observed at angle of 30° above the horizon.

The mid-latitude interaction of magnetospheric substorms with thunderstorm electricity has been firmly established. The amplitudes of spikes of positive and negative fields in the morning zone of the Earth's troposphere corresponding to the activation of substorms have been measured (~100 MV). The spikes form simultaneously at distances of 10–30 km from one another. The durations of leading edges of the positive and negative spikes are 30 s and 2 min, respectively. The characteristic energy of atmospheric electrons accelerated as a result of high-altitude impulsive discharges is estimated to be 9 MeV.

Some spikes of the positive field in the troposphere (~100 MV) in the period of substorm buildup and development in the Earth's morning sector are observed immediately before earthquakes that occur relatively nearby, at distances of 300 and 1500 km.

REFERENCES

1. Kanonidi, K.Kh., Lidvansky, A.S., Khaerdinov, M.N., and Khaerdinov, N.S., *Bull. Russ. Acad. Sci.: Phys.*, 2015, vol. 79, no. 5, p. 679.
2. Kanonidi, K.Kh., Kurenya, A.N., Lidvansky, A.S., Khaerdinov, M.N., and Khaerdinov, N.S., *Bull. Russ. Acad. Sci.: Phys.*, 2015, vol. 79, no. 5, p. 676.
3. Kanonidi, K.Kh., Lidvansky, A.S., Khaerdinov, M.N., and Khaerdinov, N.S., *Bull. Russ. Acad. Sci.: Phys.*, 2017, vol. 81, no. 2, p. 222.
4. Khaerdinov, N.S. and Lidvansky, A.S., *Proc. Int. Symp. on Thunderstorms and Elementary Particle Acceleration*, Nor-Amberd, 2015, p. 23.
5. Khaerdinov, M.N., Khaerdinov, N.S., and Lidvansky, A.S., *Bull. Russ. Acad. Sci.: Phys.*, 2017, vol. 81, no. 2, p. 246.
6. Veselovskii, B.C. and Kropotkin, A.P., *Fizika mezhplanetnogo i okolozemnogo prostranstva* (The Physics of Interplanetary and Circumterrestrial Space), Moscow: Universitetskaya Kniga, 2010.

Translated by A. Lidvansky